

000  
001  
002  
003  
004  
005  
006  
007  
008  
009  
010  
011  
012  
013  
014  
015  
016  
017  
018  
019  
020  
021  
022  
023  
024  
025  
026  
027  
028  
029  
030  
031  
032  
033  
034  
035  
036  
037  
038  
039  
040  
041  
042  
043  
044  
045  
046  
047  
048  
049  
050  
051  
052  
053

---

# The Use of Cross-Correlation Mapping in Identifying Backwards Projecting Connections between Visual Cortical Areas

---

Zack Cecere  
UCSD

## Abstract

The number of backwards projecting connections in the visual stream dwarfs the number of forward projecting connections. Yet, we have little understanding of the function of these connections. The primary obstruction to our understanding has been our inability to distinguish between the effect of feed-forward connections and feedback connections on a given neuron. In this work, I propose Cross-Correlation Mapping (CCM) as a means of isolating the effect feedback connections. Cross-Correlation Mapping is a time-embedding manifold method that has been successfully used to show unidirectional causality between two variables in complex dynamical systems [5]. I will, first, run CCM on model neural data for which we know the causal relationship to determine the effectiveness of CCM. If I can show that CCM can uncover functional connectivity in neural populations, I will use CCM and fMRI data to create a functional mapping of the feedback connections from V2 onto V1.

## 1 Introduction

The main barrier to understanding feedback connections—like the ones traveling from V2 to V1—is the difficulty of isolating the effects of feedback connections from those of other network connections. This problem is equivalent to figuring out the effect of one input connection on a neuron while many other connections are also affecting the neuron’s activity. This obviously difficult problem becomes even harder when we consider that there is no way to probe the activity of the majority of neurons feeding input into the target neuron. Cross-Correlation Mapping—a method developed in George Sugihara’s lab at Scripps Oceanographic Institute—has been successfully used to determine the causal relationship between two variables in a high-dimensional, dynamical system [5]. If we think of individual neurons as variables in a high-dimensional system—a neural network—we may guess that CCM could be used to decipher brain architecture.

## 2 Methods

### 2.1 Cross-Correlation Mapping

According to dynamical systems theory, two time-series variables are causally linked if they are from the same dynamic system [5]. For example, variables X and Y in the Lorenz attractor are causally linked because the state of X is dependent upon the previous state of Y and vice versa. We can also think of dynamical causality between two variables in terms of their shared attractor manifold. Since X is contained in the state determining equation for  $\frac{dY}{dt}$  and Y in the state determining equation for  $\frac{dX}{dt}$  in the Lorenz attractor, we know, given no change in any other variable in the system, that the X, Y phase plane will contain a coherent, well-defined attractor. If X and Y do not exhibit a causal

054 relationship, no attractor would exist—nor a phase plane, really—as the quantities  $\frac{dX}{dY}$  and  $\frac{dY}{dX}$  are  
055 undefined.

056  
057 The technique pioneered by Sugihara et al [5]—Cross-Correlation Mapping (CCM)—uses the dynamical systems definition of causality. More specifically, CCM constructs shadow manifold for two  
058 variables in the proposed system using time-lagged coordinate embedding. That is, CCM creates  
059 a shadow manifold for each variable independently. CCM creates a given point on the shadow  
060 manifold by sampling an individual variable multiple times with a fixed interval. It then checks  
061 whether nearby points in one shadow manifold correspond with nearby points in the other. There  
062 are many points that have a similar value in the parent manifold—the original manifold without any  
063 embedding—for a single variable but are not actually close to one another—that is, they have different  
064 values for the other variables. The time-lagged embedding seeks to distance these points: points not  
065 near each other on the parent manifold are unlikely to evolve through time similarly. If contiguous  
066 points in one shadow manifold can be used to identify contiguous points in another, we can build a  
067 section of a coherent higher-dimensional manifold from these contiguous points—that is, we can theoretically  
068 rebuild parts of the parent manifold from the relationship between the shadow manifolds.  
069 Thus, CCM works because a well-defined relationship between shadow manifolds indicates that a  
070 coherent attractor manifold exists in a space containing the two variables.

071 In CCM, the cross mapping between the shadow manifolds mentioned above is done for a number  
072 of library sizes. The library size is the number of points—not the dimension—used to build the shadow  
073 manifold. If the two variables related to the shadow manifolds are causally related, cross-mapping  
074 should improve with increased library size. This is because, with increased library size, there is a  
075 higher probability that the points identified as contiguous in one of the shadow manifolds actually  
076 are contiguous. Thus, the degree of convergence is the best measurement of causality in CCM  
077 analyses.

## 078 2.2 Jumbled CCM

080 The canonical methods for fMRI processing [6] output a scalar response value for each voxel to each  
081 image. Thus, we are no longer dealing with time series in fMRI data. There remains no ordering  
082 to the series as image 1 could induce a more similar overall response to image 50 than image 2. I  
083 created the jumbled CCM method to test whether the loss of a natural ordering in the data series  
084 affects CCM. Essentially, jumbled CCM works by repeatedly applying CCM while shuffling the  
085 input data. The idea is, after enough shuffles, certain points in the shadow manifold will exhibit  
086 consistent contiguity. Thus, through averaging, CCM should generate an internal representation of  
087 the true shadow manifold, despite us not actually knowing the true form of this manifold.  
088

## 089 2.3 False Neighbors Analysis

091 The minimal number of dimensions—number of time lagged values of a variable that goes into each  
092 point on the shadow manifold—that allow for the separation of points that are not near each other on  
093 the original manifold—false neighbors—is the ideal dimensionality for a time series embedding. In  
094 their 1992 paper [3], Kennel et al devised a method for finding this ideal embedding dimensionality.  
095 They hypothesized that false neighbors would distance themselves given an increase in embedding  
096 dimension.  
097

$$098 \left( \frac{R_{d+1}^2(n, r) - R_d^2(n, r)}{R_d^2(n, r)} \right) > R_{tol} \quad (1)$$

100  
101  
102 Where  $R_d$  is the euclidean distance between a given point and its nearest neighbor for dimensionality  
103  $d$ .

104 Kennel et al [3] noticed that this metric failed to parse out false neighbors with noisy data. They  
105 realized that noise causes the radius of the original manifold to increase to such a degree that the  
106 distance between every pair of points in the embedded manifold for a given series is very large. In  
107 order to account for this, they devised a metric that compares the distance between two points in a  
given embedding dimension to the radius of the attractor.

108  
109  
110  
111  
112  
113  
114  
115  
116  
117  
118  
119  
120  
121  
122  
123  
124  
125  
126  
127  
128  
129  
130  
131  
132  
133  
134  
135  
136  
137  
138  
139  
140  
141  
142  
143  
144  
145  
146  
147  
148  
149  
150  
151  
152  
153  
154  
155  
156  
157  
158  
159  
160  
161

$$\frac{R_{d+1}(n)}{R_A} > A_{tol} \tag{2}$$

The idea is that false neighbors will be kicked out to the edge of the attractor by adding additional embedding dimensions.

Typically, the method of false neighbors outputs, as one would expect, the number of nearest neighbors found to be false by increasing the dimensionality by one. In this study, I simply calculate the values of metrics 1 and 2 averaged across a number of points for a number of dimensions, assuming that these metrics are proportional to the number of false neighbors.

## 2.4 Granger Causality

Granger causality, in its simplest form, uses linear-autoregression to determine whether the value of one variable can be predicted from another.

$$X_1(t) = \sum_{j=1}^p A_{11,j} X_1(t-j) + \sum_{j=1}^p A_{12,j} X_2(t-j) + E_1(t) \tag{3}$$

In the above example, variable X2 Granger-causes variable X1 if the variance of E1 is reduced by the inclusion of X2 in the first term [2]. When the variance of the error term E1 decreases in this way, we know that we can use X2 to better predict the statistical structure of X1. Granger causality and CCM are similar in the respect that they measure how well the statistical structure of one variable can be used to predict that of another. The primary difference between the two methods is that CCM is tuned for and gives more information about any manifold that may pass through the space encompassing the two variables.

We implemented two forms of Granger causality. Our first-order implementation simply uses the responses of a variable number of voxels to about 1000 natural images to predict the behavior of another voxel to the same images using least-squares optimization. This method then stores the variance of the prediction error. We also implemented a second-order Granger causality method that considers correlations between the input voxels in addition to the raw values of the input voxels. The second-order method exhibited superior performance but proved to be too slow to use—unparallelized—for large data sets.

## 3 Results

### 3.1 Testing CCM on Chaotic Data

In order to determine whether CCM works at all, we tested the method on several chaotic systems. First, we used a simple, two-state chaotic system with variable causality strength between the two variables.

Since the CCM result converges for the non-zero causality case and not for the zero causality case, we know that CCM is able to identify causality for simpler chaotic systems.

Sugihara et al [5] claimed that CCM could determine the direction of causality between two variables. We tested this claim using a modified form of the previously mentioned chaotic model. In this new version of the chaotic model, variable X has a causal effect on variable Y but variable Y does not have a causal effect on variable X.

The contrasting results in figures 2 and 3 indicate that CCM is, in fact, able to determine the direction of causality between two variables.

Most interesting systems have many interacting variables. In order for CCM to be useful, it must have the ability to identify causality between pairs of variables in these complex systems. We tested CCM’s ability to find causal relationships in these complex systems using a 5-state chaotic model in which only certain variables are causally related.

162  
 163  
 164  
 165  
 166  
 167  
 168  
 169  
 170  
 171  
 172  
 173  
 174  
 175  
 176  
 177  
 178  
 179  
 180  
 181  
 182  
 183  
 184  
 185  
 186  
 187  
 188  
 189  
 190  
 191  
 192  
 193  
 194  
 195  
 196  
 197  
 198  
 199  
 200  
 201  
 202  
 203  
 204  
 205  
 206  
 207  
 208  
 209  
 210  
 211  
 212  
 213  
 214  
 215

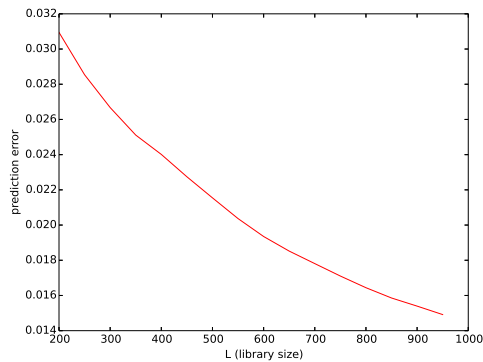


Figure 1: Results of a CCM run on two variables in a chaotic model known to exhibit dynamic causality. The improvement of prediction with library size indicates that CCM correctly identifies this causal relationship.

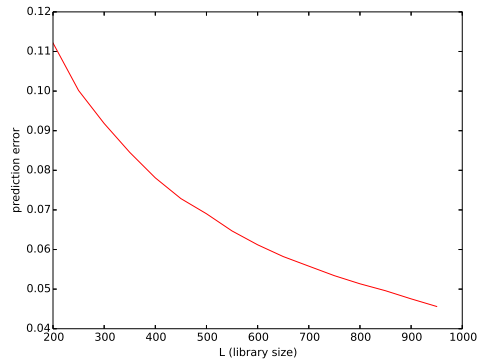


Figure 2: CCM test in the direction of  $X \rightarrow Y$ . The improving performance of CCM with library size shows that CCM correctly identifies X as causing the behavior of Y.

CCM correctly identifies variables 2 and 3 as causing the behavior of variable 1. It also correctly shows—via a lack of improvement in correlation index (inverse of prediction error)—that variable 4 does not cause the behavior of variable 1. This result is very encouraging as it allows us to apply CCM to high dimensional neural systems.

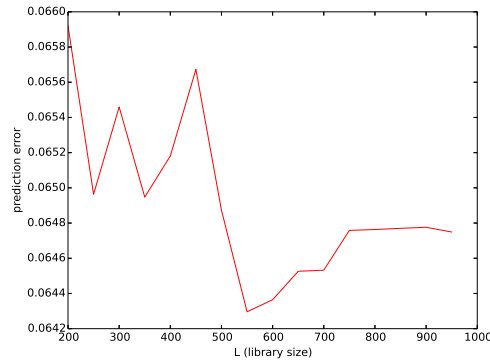
### 3.2 Testing CCM on Hodgkin-Huxley Networks

Given that we can describe most neural systems with dynamical equations, we expect to be able to apply CCM to neural data. More specifically, we wish to apply CCM on the level of neurons and neuronal populations, finding causally related—aka, functionally connected—neurons and neuronal populations. To test whether we can apply CCM in this way, we generated the following sample feed-forward model composed of Hodgkin-Huxley neurons:

Several interesting observation arose in the analysis of this network. First, we notice that CCM identifies neuron 0 as being functionally connected to neurons 2, 5, and 6—evidenced by the convergence in figures 5, 6, and 7.

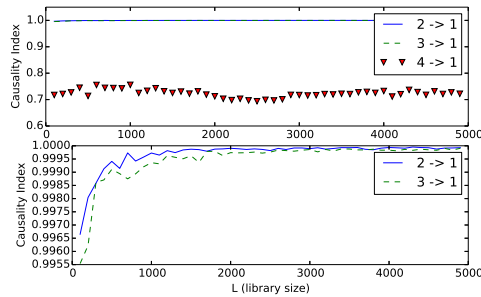
Although neuron 0 is technically only connected to neuron 2, the fact that CCM identifies it as being functionally connected to neurons 5 and 6 is both useful and correct. Neuron 0, through neuron 2, singularly controls the behavior of neuron 5, and controls the behavior of neuron 6 in concert with neuron 1. Moreover, the CCM output converges to the lowest value in the case of the  $0 \rightarrow 2$

216  
217  
218  
219  
220  
221  
222  
223  
224  
225  
226  
227  
228  
229



230 Figure 3: CCM test in the direction of  $Y \rightarrow X$ . One could make the claim that this figure shows  
231 convergence. However, the level of improvement with library size, in this case, is not above chance,  
232 indicating the CCM correctly shows there to be no causal effect of Y on X.  
233

234  
235  
236  
237  
238  
239  
240  
241  
242  
243  
244



245 Testing the effectiveness of CCM on chaotic model where variable 1 causally  
246 affects variables 2 and 3, but not variable 4. CCM correctly recognizes these  
247 causalities as only the 2->1 and 3->1 connections' causality indices  
248 converge to 1. Note: the second plot is a zoomed in version of the first.

249  
250  
251

252 connection, providing us with a means of separating the tiers of connectivity. Thus, in the case of  
253 neural data, the consistently decreasing / converging behavior of CCM output identifies functional  
254 connectivity—further evidenced by the lack of convergence in the  $0 \rightarrow 4$  CCM run—while the  
255 values at convergence allow for the ranking of connectivities in a network.

256 In our testing of various network architectures, we found that CCM struggles to identify only one  
257 connection type. If a given Hodgkin-Huxley neuron receives an input from only one other neuron,  
258 CCM cannot not deduce whether the connection projects onto the given neuron or from the given  
259 neuron. For example, CCM was unable to determine the directionality of the connection between  
260 neurons 0 and 2 in the above network.

261 Although CCM suggests that neuron 0 synapses onto neuron 2 and vice versa, it performs much  
262 better—in terms of noise of the curve and converged prediction error—in the correct direction—the 0 to  
263 2 direction. This sparsely connected case will likely not matter in real neural data because real neural  
264 networks are much more highly connected and noisy than our Hodgkin-Huxley simulations. How-  
265 ever, this failure of CCM requires us to apply CCM in both directions for a hypothetical connection  
266 in order for us to be certain of the directionality of the connection.

267  
268  
269

267 Thus far, we have demonstrated that we can easily apply CCM on the level of small networks.  
268 However, CCM would prove even more useful if we could apply it on the level of large-scale brain  
269 dynamics. To this end, we will attempt to use CCM in conjunction with fMRI data to gain some  
insight on large-scale connectivity in the visual cortex.

270  
271  
272  
273  
274  
275  
276  
277  
278  
279  
280  
281  
282  
283  
284  
285  
286  
287  
288  
289  
290  
291  
292  
293  
294  
295  
296  
297  
298  
299  
300  
301  
302  
303  
304  
305  
306  
307  
308  
309  
310  
311  
312  
313  
314  
315  
316  
317  
318  
319  
320  
321  
322  
323

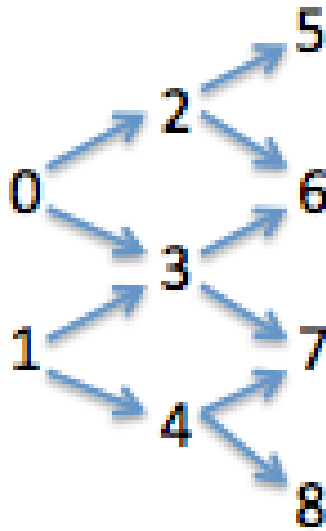


Figure 4: The network used to generate the Hodgkin-Huxley data.

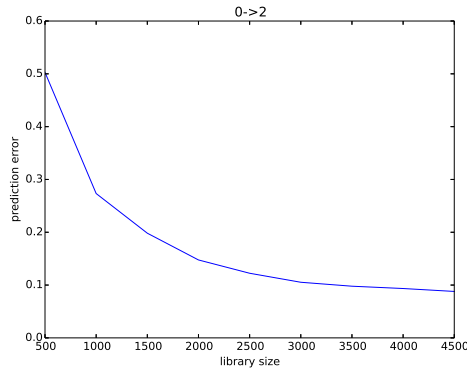


Figure 5: CCM correctly identifies a functional connection from neuron 0 to neuron 2.

### 3.3 Applying CCM to fMRI Data

Thus far, we have demonstrated that we can apply CCM on the level of small networks. However, CCM would prove even more useful if we could apply it on the level of large-scale brain dynamics. To this end, we will attempt to use CCM in conjunction with fMRI data to gain some insight on large-scale connectivity in the visual cortex.

We obtained visual cortical fMRI data from the Gallant lab [6]. The Gallant lab generated the data by taking fMRI reading from humans viewing natural scenes. The response of each voxel to each image was determined using the hemodynamic response convolution protocol discussed in [6]. Since the protocol assumes that each voxel has a scalar response—more specifically, a scale on the unchanging HRF of the voxel—to a given image, it outputs data that is not a time series. To deal with this unordered data, we created the jumbled CCM method.

Before applying the jumbled CCM method to fMRI data, we tested the method’s validity on the chaotic and Hodgkin-Huxley data already discussed.

324  
325  
326  
327  
328  
329  
330  
331  
332  
333  
334  
335  
336  
337  
338  
339  
340  
341  
342  
343  
344  
345  
346  
347  
348  
349  
350  
351  
352  
353  
354  
355  
356  
357  
358  
359  
360  
361  
362  
363  
364  
365  
366  
367  
368  
369  
370  
371  
372  
373  
374  
375  
376  
377

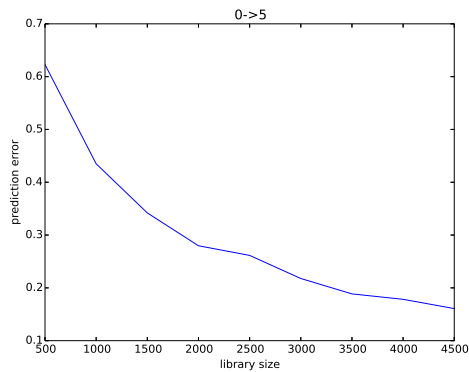


Figure 6: CCM correctly identifies a functional connection from neuron 0 to neuron 5, despite the fact that neuron 5 is two edge lengths away.

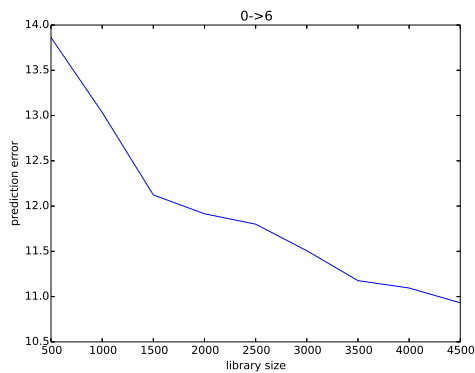


Figure 7: CCM correctly identifies a functional connection from neuron 0 to neuron 6. This is an especially encouraging result as neuron 6 receives information from both neuron 0 and neuron 1—two neurons with very different activities.

In the methods section, we hypothesized that the jumbled CCM method could generate an internal representation of the shadow manifolds of the two input variables, despite us not knowing the true form of these manifolds. The success of the jumbled CCM in regenerating our earlier data—both the chaotic and Hodgkin-Huxley models (data not shown)—indicates that this hypothesis has merit.

Before moving on to the fMRI analysis, we needed to determine the embedding dimension our CCM method should use. As discussed in the methods section, using too low of an embedding dimension will often produce false neighbors. We used the method of false neighbors to determine the optimal embedding dimension [3].

After applying the method of false neighbors to voxel 100 of V1 in the fMRI data—the central voxel of our study—we decided to use an embedding dimension of 70.

Due to the many averaging steps required in jumbled CCM, the method is very slow. Thus, we decided that, for the sake of time (and the fact that I ran all of the simulations on a MacBook Pro) that we would analyze how the behavior of only voxel 100 in V1 (primary visual cortex) is controlled by voxels in V2.

In figure 13, we see that a small region of V2—from about voxel 200 to voxel 300—exhibits a compressed range of values to which the CCM prediction error converges. This trend becomes more obvious when we average the values of nearby voxels (figure 14). Thus, there exists some indication that this area of V2 project backs to voxel 100 in V1.

378  
379  
380  
381  
382  
383  
384  
385  
386  
387  
388  
389  
390  
391  
392  
393  
394  
395  
396  
397  
398  
399  
400  
401  
402  
403  
404  
405  
406  
407  
408  
409  
410  
411  
412  
413  
414  
415  
416  
417  
418  
419  
420  
421  
422  
423  
424  
425  
426  
427  
428  
429  
430  
431

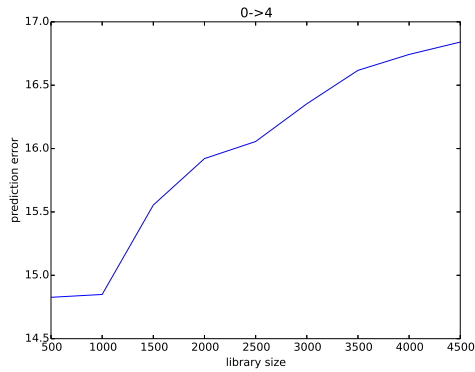


Figure 8: CCM correctly identifies the lack of a functional connection from neuron 0 to neuron 4.

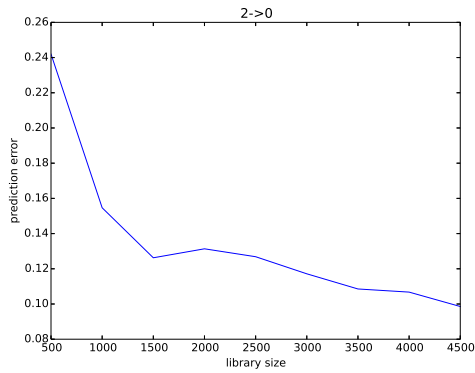


Figure 9: CCM falsely finds a connection from neuron 2 to neuron 0. This is a result of neuron 2's behavior being totally determined by the behavior of neuron 0.

In order to validate our hypothesis that voxels in the 200-300 region project back to voxel 100 in V1, we tested CCM exhaustively on voxels in this region. More specifically, we averaged thousands of jumbled CCM trials, attempting to eliminate as much noise as possible. We believed that this method was effective because every massively averaged CCM run on the same two voxels produced the same library size vs. prediction error figure. Figure 15 shows the massively averaged CCM output for the hypothetical connection from voxel 215 in V2 onto voxel 100 in V1.

Figure 15 strongly suggests that voxel 215 in V2 projects onto voxel 100 in V1. In fact, if we assume every change in prediction error due to the addition of new points for consideration has a 50:50 chance of being negative—as is the case in CCM analyses of random data (data not shown)—the binomial theorem indicates that there is less than a 5 percent chance of obtaining as many decreases with increasing library size as seen in figure 15. Coupling this analysis with the fact that many of the voxels near 215 show similar relationships with voxel 100 in V1, we believe that this region of V2 projects back to V1.

We discovered in our Hodgkin-Huxley analysis that CCM sometimes struggles in determining the directionality of a connection. Keeping this in mind, we ran CCM to determine whether voxel 100 in V1 projects onto voxel 215 in V2.

Figure 16 gives no indication of voxel 100 in V1 projecting onto voxel 215 in V2. This further supports our result: voxel 215, as well as other nearby voxels in V2, projects functional connections back to voxel 100 in V1.



432  
433  
434  
435  
436  
437  
438  
439  
440  
441  
442  
443  
444  
445  
446  
447  
448  
449  
450  
451  
452  
453  
454  
455  
456  
457  
458  
459  
460  
461  
462  
463  
464  
465  
466  
467  
468  
469  
470  
471  
472  
473  
474  
475  
476  
477  
478  
479  
480  
481  
482  
483  
484  
485

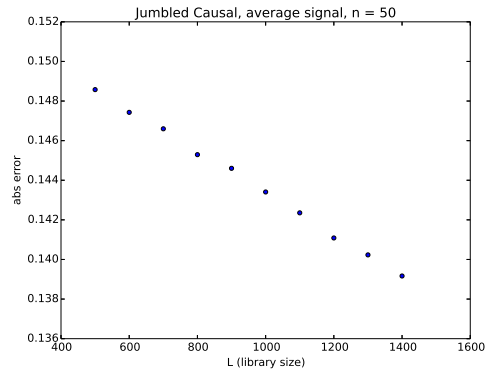


Figure 10: The jumbling does not interfere with CCM’s ability to identify a causal connection; it still recognizes dynamical causality in this chaotic model.

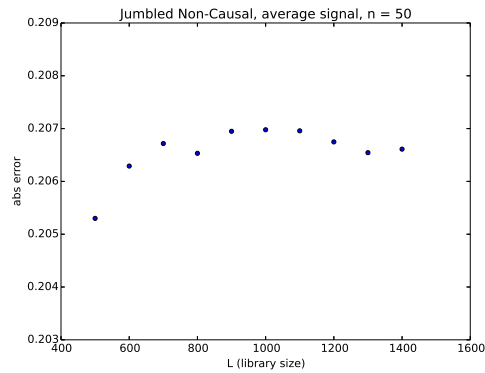


Figure 11: The jumbling does not interfere with CCM’s ability to identify the lack of a causal connection. This was done for two un-related variables in a high-order, chaotic model.

Thus, our data recommends that the response of voxel 100 in V1—and likely many other voxels in V1—is influenced in a dynamically causal manner by a population of voxels in V2.

### 3.4 Comparison to Granger Causality

In the hope of amassing more evidence for functional backwards-projecting connections from V2 to V1, we implemented a form of Granger causality. More specifically, we used a first-order Granger causality method (Methods) to determine which V2 voxels best predict the behavior of voxel 100 in V1.

Our scan of V2 voxels that Granger cause’ the behavior of voxel 100 in V1 produced similar—but certainly not identical—results to those of CCM. One interesting result of the Granger causality scan is that, on average, the voxels around voxel 215 of V2 predicted the statistical properties of voxel 100 in V1 most accurately. This directly agrees with the CCM analysis. However, the Granger causality scan indicates that the V2 region around voxel 75 can also be used to accurately predict the behavior of voxel 100 in V1. The CCM analysis unearthed no such pattern.

## 4 Conclusion

Our Hodgkin-Huxley analysis shows that Cross-Correlation Mapping is a valid technique for determining functional connectivity in small neural networks. Moreover, the fact that CCM performance

486  
 487  
 488  
 489  
 490  
 491  
 492  
 493  
 494  
 495  
 496  
 497  
 498  
 499  
 500  
 501  
 502  
 503  
 504  
 505  
 506  
 507  
 508  
 509  
 510  
 511  
 512  
 513  
 514  
 515  
 516  
 517  
 518  
 519  
 520  
 521  
 522  
 523  
 524  
 525  
 526  
 527  
 528  
 529  
 530  
 531  
 532  
 533  
 534  
 535  
 536  
 537  
 538  
 539

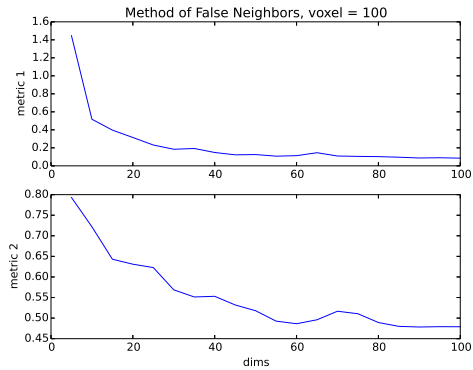


Figure 12: Results of method of false neighbor analysis on voxel 100 in V1 of the fMRI data. The y-axis in the top figure is equation 1, while the y-axis on the bottom figure is equation 2 (methods). Together, the figures indicate that we cease to gain a benefit—root out false neighbors—from increased embedding dimensionality at about 65 dimensions.

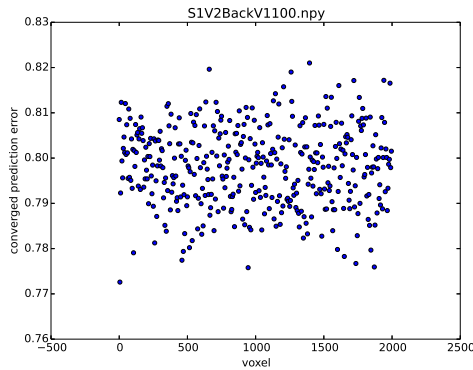


Figure 13: Results of running CCM to determine which voxels in V2 (V2 voxel number shown on x-axis) causally effect the behavior of voxel 100 in V1. The y-axis is the value to which the CCM run converged. We used converged value for this figure because the value to which a CCM run converges is stable between CCM runs. The initial behavior of the CCM output, however, requires the averaging of many CCM runs to gain a stable shape. Thus, we could only analyze the initial behavior for a small number of voxels.

actually improves with more connectivity and noise suggest that CCM can be applied to all types of neural data. Indeed, our application of CCM to visual cortical fMRI data provided very strong evidence for the existence of backpropagating information. This finding is a very nice support for the predictive coding model of visual processing [4].

Although we achieved some success in our use of CCM, the jumbling method we were forced to use in our fMRI analysis was both slow and noise inducing. We are currently working on applying the maximum noise entropy method [1] to find the visual features to which each voxel in a number of visual areas responds. We will then apply these voxel response models to a number of slowly morphing visual stimuli to obtain intrinsically ordered data—that is, stimulus 1 will be more similar to stimulus 2 than to stimulus 50. This method should grant us a representation of the shadow manifolds without the need for jumbling.

540  
 541  
 542  
 543  
 544  
 545  
 546  
 547  
 548  
 549  
 550  
 551  
 552  
 553  
 554  
 555  
 556  
 557  
 558  
 559  
 560  
 561  
 562  
 563  
 564  
 565  
 566  
 567  
 568  
 569  
 570  
 571  
 572  
 573  
 574  
 575  
 576  
 577  
 578  
 579  
 580  
 581  
 582  
 583  
 584  
 585  
 586  
 587  
 588  
 589  
 590  
 591  
 592  
 593

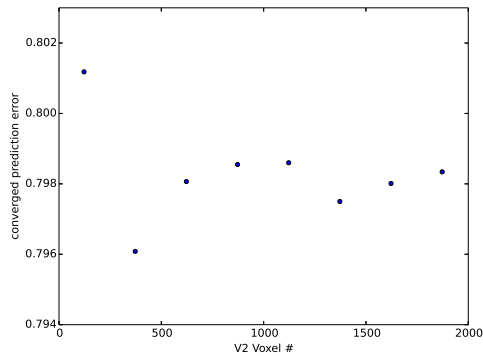


Figure 14: What happens after we average the converged values of nearby voxels (essentially, binned the results of figure 12). Here, we see more clearly the dip in CCM converged value in the 200-300 voxel section.

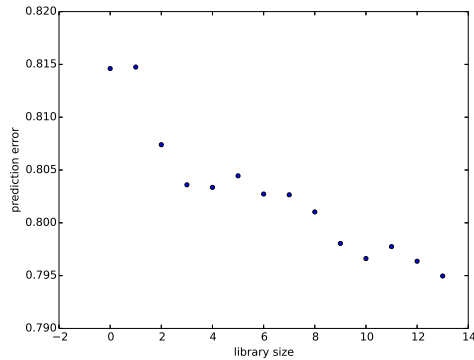


Figure 15: The signal produced by the averaging of many CCM runs testing whether voxel 215 in V2 functionally causes the behavior of voxel 100 in V1. The fact that pretty much every set of averaged CCM runs for this voxel combination converges to this improving estimation pattern strongly advocates for a function connection from voxel 215 in V2 to voxel 100 in V1.

## 5 References

[1] Fitzgerald et al. Second Order Dimensionality Reducton Using Minmum and Maximum Mutual Information Models. PLoS Computational Biology 7. (2011).

[2] Granger, C. W. J. Investigating causal relations by econometric models and cross-spectral methods. Econometrica 37. 424-438 (1969).

[3] Kennel, Brown, and Abarbanel. Determining embedding dimension for phase-space reconstruction using geometrical construction. Physical Review A 45. (1992).

[4] Rao and Ballard. Predictive coding in the visual cortex: a functional interpretation of some extra-classical receptive-field effects. Nature Neuroscience 2. (1999).

[5] Sugihara et al. Detecting Causality in Complex Ecosystems. Science 338. (2012).

[6] Kay et al. Identifying natural images from human brain activity. Nature 452. (2008).

594  
595  
596  
597  
598  
599  
600  
601  
602  
603  
604  
605  
606  
607  
608  
609  
610  
611  
612  
613  
614  
615  
616  
617  
618  
619  
620  
621  
622  
623  
624  
625  
626  
627  
628  
629  
630  
631  
632  
633  
634  
635  
636  
637  
638  
639  
640  
641  
642  
643  
644  
645  
646  
647

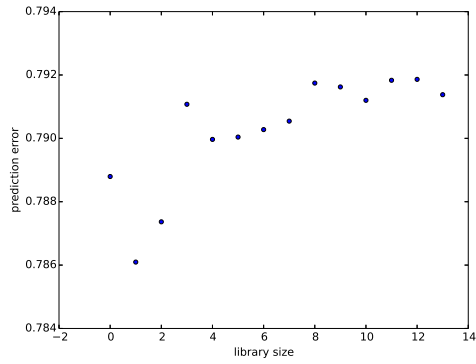


Figure 16: We used the same averaging of CCM runs technique here that we used for figure 14. The loss of performance with increasing library size indicates that there is no little causal connectivity from voxel 100 in V1 to voxel 215 in V2.

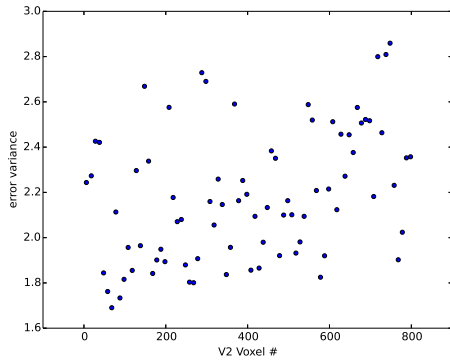


Figure 17: Each point corresponds with a prediction of the behavior of voxel 100 in V2 from 30 voxels in V2 starting at the x-value of the point.

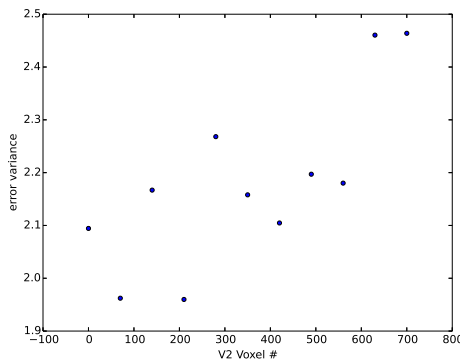


Figure 18: This figure was generated by binning the previous figure.